Published in final edited form as:
Anal Chem. 2013 June 18; 85(12): 6066–6072. doi:10.1021/ac400932s.

Microfluidic Amperometric Sensor for Analysis of Nitric Oxide in Whole Blood

Rebecca A. Hunter[*], **Benjamin J. Privett**[*], **W. Hampton Henley**[*], **Elise R. Breed**[†,‡], **Zhe Liang**[†,‡], **Rohit Mittal**[†,‡], **Benyam P. Yoseph**[†,‡], **Jonathan E. McDunn**[§], **Eileen M. Burd**[#], **Craig M. Coopersmith**[†,‡], **J. Michael Ramsey**[*,§], and **Mark H. Schoenfisch**[*]

[*]Department of Chemistry, University of North Carolina at Chapel Hill, Chapel Hill, North Carolina 27599

[†]Emory Center for Critical Care, Emory University School of Medicine, Atlanta, Georgia 30322

[‡]Department of Surgery, Emory University School of Medicine, Atlanta, Georgia 30322

[§]Department of Biomedical Engineering, University of North Carolina at Chapel Hill, Chapel Hill, North Carolina 27599

[#]Department of Pathology and Laboratory Medicine, Emory University School of Medicine, Atlanta, Georgia 30322

Abstract

Standard photolithographic techniques and a nitric oxide (NO) selective xerogel polymer were utilized to fabricate an amperometric NO microfluidic sensor with low background noise and the ability to analyze NO levels in small sample volumes (~250 μL). The sensor exhibited excellent analytical performance in phosphate buffered saline, including a NO sensitivity of 1.4 pA nM^{-1}, a limit of detection (LOD) of 840 pM, and selectivity over nitrite, ascorbic acid, acetaminophen, uric acid, hydrogen sulfide, ammonium, ammonia, and both protonated and deprotonated peroxynitrite (selectivity coefficients of −5.3, −4.2, −4.0, −5.0, −6.0, −5.8, −3.8, −1.5, and −4.0 respectively). To demonstrate the utility of the microfluidic NO sensor for biomedical analysis, the device was used to monitor changes in blood NO levels during the onset of sepsis in a murine pneumonia model.

Keywords

Nitric oxide; amperometric sensor; microfluidic device; sensor membrane; sepsis

Introduction

Nitric oxide (NO), a diatomic free radical endogenously produced by a class of enzymes known as nitric oxide synthases (NOS),[1–9] plays a role in a number of physiological processes including wound healing,[10–12] angiogenesis,[13–16] and the immune response.[17–19] As might be expected, the detection and quantification of NO in vivo and from NO donor scaffolds have been the subject of intense research.[20–27] Measuring NO in biological systems is challenging due to NO's reactivity (i.e., short half-life), wide concentration range

schoenfisch@unc.edu.

COMPETING FINANICIAL INTETEREST. The authors declare competing financial interest. Mark Schoenfisch is a founder, member of the board of directors, and maintains a financial interest in Clinical Sensors, Inc. Clinical Sensors, Inc. is developing point-of-care sepsis risk assessment devices.

(pM to μM),[1–3, 28] and sample complexity.[20] Despite such challenges, direct and indirect methods for measuring NO are routinely employed to determine its concentration in biological samples.[23] Often, NO is most easily quantified by measuring its oxidative byproducts (e.g., nitrite and nitrate). In this respect, absorbance or fluorescence may be used to quantify NO upon its reaction with an assay reagent after oxidation to nitrite or nitrate (i.e., NO_X).[3, 29–31] Depending on the sample, pre-existing NO_X species could be measured simultaneously and thus must be considered when determining the signal from solely NO. For example, the Griess assay is widely used to quantify NO indirectly as nitrite in solution. Nitrite and nitrate levels fluctuate in physiological milieu,[1–3, 28] making real-time NO concentration determination complex.[3] Strategies for measuring NO more directly include chemiluminescence,[32, 33] electron paramagnetic resonance (EPR) spectroscopy,[21, 32, 34] and the use of electrochemical sensors.[20, 23] Although measurement of NO by chemiluminescence or EPR allows for sensitive and direct analysis, the required instrumentation for these methods is expensive, requires extensive user training, and is difficult to adapt for analysis of challenging biological matrices such as whole blood.[35, 36] In contrast, electrochemistry allows for real-time measurement of NO in physiological media using a sensor platform that is tunable (i.e., sensor style, geometry, material, and size) based on the application at a generally low cost.[20, 21, 23, 24, 34, 37–50] For biomedical use, electrochemical sensors are amenable to miniaturization and thus can facilitate both in vivo and ex vivo analysis.[20, 21, 51, 52]

A notable obstacle for measuring NO accurately in biological milieu via amperometry is the presence of interfering species such as nitrite, acetaminophen, ascorbic acid, uric acid, hydrogen sulfide, ammonium/ammonia, and peroxynitrite that may also be redox active at the working electrode potential required for NO analysis.[20, 53, 54] Almost all effective NO sensor designs include a membrane-modified working electrode to eliminate or reduce the diffusion of interferents and concomitant erroneous sensor response. For example, working electrodes have been modified with Teflon,® Nafion,® and silicon rubber membranes to restrict the diffusion of nitrite and larger molecules such as dopamine and ascorbic acid to the electrode surface, relative to NO.[45, 46, 52, 55] To simplify NO sensor fabrication, we have employed xerogel sensor membranes that enable straightforward modification of a number of electrode geometries via dip-coating or casting of a sol solution.[47, 48] The ensuing xerogel-modified sensors are characterized by superior analytical performance (i.e., sensitivity and selectivity for NO).

The style of electrode platform (i.e., needle-type, planar, microfluidic) is dependent on the intended measuring environment. For example, needle-type sensors provide adequate NO sensitivity for single cell analysis.[44, 49] The sensor design requirements for blood analysis are more complex. Malinski et al. reported the fabrication of a Teflon®-coated NO microsensor (5 μm tip diameter) to measure NO intravascularly in human subjects before and after the administration of bradykinin.[49] However, the clinical utility of such in vivo devices proved poor primarily due to biofouling (i.e., protein adsorption, platelet adhesion, and clot formation) that leads to erratic or unreliable sensor response.[56] While ex vivo measurements are possible, the most common sensor designs require large sample volumes (>1 mL) and convection that increases background noise and negatively impacts analytical performance.

In contrast to stand-alone sensors, the use of microfluidics allows for reduced sample volume and handling (e.g., elimination of mechanical convection), thus addressing the shortcomings of prior devices and analytical methodology required for clinical analysis.[57, 58] With respect to NO, Spence et al. combined microfluidics with planar carbon ink electrodes to measure NO from stimulated endothelial cells.[59] The device was fabricated using polydimethylsiloxane (PDMS) channel walls. Recognizing that NO and other gases may

diffuse through PDMS, Cha et al. reported the fabrication of a catalytic gold/indium tin oxide microfluidic NO sensor using polyethylene tetraphthalate/polyurethane channels to minimize loss of NO.[60] Despite suitable analytical performance in phosphate buffered saline (PBS; 10 pA nM^{-1} NO), the design of this device was complex, requiring hand assembly.

Herein, we report the use of sol-gel chemistry and standard photolithographic techniques amenable to rapid, reproducible, and inexpensive fabrication of microfluidic NO sensors. The analytical performance of the device is demonstrated in simulated wound fluid and whole blood, indicating the ability to measure NO in complex media. Toward more clinical applications, the device is used to monitor NO concentrations in a murine model of sepsis confirming that NO levels increase during a systemic inflammatory response to infection.[2, 3]

Materials and Methods

(Heptadecafluoro-1,1,2,2-tetrahydrodecyl)trimethoxysilane (17FTMS) was purchased from Gelest (Tullytown, PA). Methyltrimethoxysilane (MTMOS), (3-aminopropyl)triethoxysilane (APTES), ascorbic acid, acetaminophen, sodium sulfide and sodium nitrite were purchased from Sigma (St. Louis, MO). Ammonium hydroxide solution (14.8 M) was purchased from Fisher Scientific (Hampton, NH). Nitric oxide gas (99.5%) was purchased from Praxair (Danbury, CT). Nitrogen and argon gases were purchased from National Welders Supply (Raleigh, NC). Other solvents and chemicals were analytical-reagent grade and used as received. A Millipore Milli-Q UV Gradient A10 System (Bedford, MA) was used to purify distilled water to a final resistivity of 18.2 MΩ·cm and a total organic content of <6 ppb. Simulated wound fluid was produced by diluting fetal bovine serum (FBS) obtained from Sigma in distilled water (1:10, v:v). Whole porcine blood was drawn into 1:10 (v:v) 40 mM ethylenediaminetetraacetic acid (EDTA) from healthy pigs at the Francis Owen Blood Lab (University of North Carolina, Chapel Hill, NC).

Preparation of working electrodes

Planar platinum (Pt) electrodes were patterned onto on a 0.9 mm thick SCHOTT B270 glass substrate (Telic Company; Valencia, CA) via photolithography and evaporative metal deposition. Glass substrates (100 × 100 mm) were cleaned with distilled water, isopropanol, nitrogen gas, and then dried at 95 °C for 5 min. After cooling to room temperature, Microposit S1813 photoresist (Microchem Corp.; Newton, MA) was deposited via spincoating at 3000 rpm for 45 s. The substrate was then soft-baked at 115 °C for 2 min. An electrode pattern was exposed through a polyester film/emulsion photomask (Infinite Graphics Incorporated; Minneapolis, MN) for 10 s using a Karl SÜSS MA6/BA6 mask aligner (hard contact, 100 μm gap) equipped with a 350 W UV lamp (SÜSS Microtec; Garching, Germany). The pattern was developed in an AZ400 alkaline developer (1:3 dilution in water) for 1 min, rinsed with distilled water, dried with nitrogen gas, and then baked on a hotplate at 115 °C for 2 min. The exposed glass surface was oxygen plasma cleaned at 100 W for 1 min. To fabricate working electrodes, 10 nm Ti and 150 nm Pt were deposited in a Kurt J. Lesker PVD 75 magnetron sputtering system (Clairton, PA). The substrate was soaked in acetone to liftoff the remaining photoresist and excess metal resulting in 100 μm wide patterned Pt electrodes on glass.

Membrane synthesis and deposition

Working electrode-modified glass substrates were rinsed with distilled water, dried with nitrogen, and heated at 95 °C for 5 min. Substrates were then oxygen plasma cleaned at 100 W for 1 min. The membrane deposition regions were masked by evenly applying 1002F-50 photoresist (prepared as previously described[61]) by spin-coating at 500 rpm for 10 s, 3000 rpm for 40 s, and heating at 95 °C for 1 h on a hot plate. The electrode pattern was exposed

through a chrome mask for 80 s using the mask aligner. Following exposure, the substrate was baked on a hot plate at 95 °C for 10 min. The pattern was developed in SU-8 developer (Microchem Corp.; Newton, MA) for 6 min, rinsed with isopropanol, dried with nitrogen, and baked on a hotplate at 115 °C for an additional 10 min. An adhesion layer of APTES was deposited via three 5 mL injections at 130 °C using a LabKote vapor deposition system (Yield Engineering Systems; Lawrence, CA). The fluoroalkoxysilane membrane solution was prepared via the acid catalyzed hydrolysis and condensation of 17FTMS and MTMOS as reported previously.[47] Briefly, 600 μL absolute ethanol, 120 μL MTMOS, 30 μL 17FTMS, 160 μL distilled water, and 10 μL 0.5 M HCl were added sequentially to a 1.5 mL microcentrifuge tube with vigorous mixing between the addition of each component. This solution was then vortexed for 1 h. Working with 16 electrode batches, 30 μL of the sol solution was spread-cast across the working electrodes using a pipette tip for 1 min to ensure even coating. The xerogel-coated substrate was then dried overnight under ambient conditions to facilitate adequate curing. The 1002F-50 photoresist was removed by soaking the substrate for 1 h in distilled water. Membrane thickness was characterized using a P15 Profilometer (KLA-Tencor Corp.; San Jose, CA).

Microfluidic device fabrication

Reference electrodes were fabricated on separate glass microscope slides. The slides were oxygen plasma cleaned (100 W, 5 min) and masked with tape so that only the middle third of each slide remained exposed. Reference electrodes were deposited in this region by first sputtering a 10 nm Ti adhesion layer followed by a ~1 μm Ag layer in the magnetron sputtering system. To form channel walls, two parallel strips of 6.3 mm double-sided Kapton® polyimide tape (90 μm thick, KaptonTape.com) were applied ~3 mm apart and perpendicular to the Pt electrodes on the working electrode substrate. The reference electrode slide was then bonded to the working electrode substrate (reference electrode facing down) by aligning and clamping the components together with spring clamps and heating at 100 °C for 5 min. After the ends of the channel were sealed, 8 mm diameter inlet/outlet reservoirs were affixed to the device using a high-strength, chemical-resistant epoxy (Loctite® Professional Heavy Duty 5 min; Westlake, OH). Electrical wires were soldered directly to the solder-on pads of each electrode facilitating an electrical connection to the potentiostat. Prior to using the device to measure NO, the Ag electrode was chemically oxidized by reaction in 50 mM ferric chloride for 10 s to create a pseudo-reference/counter electrode. Following this process, the device channel was rinsed with distilled water.

Microfluidic device characterization

To evaluate the performance of the microfluidic device, the working and reference/counter electrodes were connected to a CH Instruments 1030A 8-channel potentiostat (Austin, TX). Gravity solution flow (~100 μL min^{-1}) was employed to move sample through the device by attaching a 40 mm piece of Tygon® tubing to the inlet reservoir. This location served as the introduction site. Prior to sample analysis, the device was polarized at 700 mV vs. the Ag/AgCl pseudo-reference/counter electrode for up to 1 h in PBS. To calibrate the device, a saturated NO standard solution (prepared by purging deaerated PBS with NO gas for ~10 min resulting in a 1.9 mM solution of NO) was diluted with PBS and introduced into the inlet reservoir. To assess the selectivity of the sensor for NO, separate solutions of nitrite, acetaminophen, ascorbic acid, uric acid, hydrogen sulfide, ammonia/ammonium, and peroxynitrite (protonated and deprotonated) were injected into the device. The sensitivity of the microfluidic sensor to NO was also tested in both simulated wound fluid (10% v/v fetal bovine serum in water) and anti-coagulated porcine whole blood. In these experiments, select volumes of the saturated NO solution were added to 2 mL aliquots of blood, mixed briefly, and added to the sample reservoir. For wound fluid testing, increasing volumes of

saturated NO were added to 30 mL of wound fluid, mixed, and added to the sample reservoir.

Animals

Murine sepsis experiments were performed using C57Bl6/J mice that had free access to food and water, and were maintained on a 12 h light/dark schedule. Animal studies were performed in accordance with National Institutes of Health Guidelines and approved by the Emory University Institutional Animal Care and Use Committee (IACUC). To initiate pneumonia-induced sepsis, mice were anesthetized using isoflurane and then received a mid-line cervical incision. A total of 40 μL of *Pseudomonas aeruginosa* (ATCC 27853) suspended in normal saline was then introduced by direct intratracheal installation using a 28-gauge needle, corresponding to 2–4 x 10^7 colony-forming units.[62, 63] To enhance delivery of the bacteria into the lungs, mice were held vertically for 10 s. All mice received a subcutaneous injection of saline (1 mL) post-operatively to compensate for insensible fluid losses. For NO measurement, 250 μL of blood was obtained via cardiac puncture (while the animals were under anesthesia) at the time of sacrifice. The blood was immediately transferred to an EDTA tube, mixed, and injected onto the sample port of the microfluidic device. Blood samples from unmanipulated mice in the absence of bacteria exposure were used as the 0 h time point for NO analysis and evaluated throughout the experiment as controls. Additionally, all sensors were calibrated before, during, and after animal experiments.

Statistical analysis

Murine sepsis data were analyzed using OriginPro 7.0 (OriginLab; Northampton, MA) and presented as mean ± standard error of the mean. Comparisons between groups were performed using the Wilcoxon rank-sum test with $P < 0.05$ considered to be statistically significant.

Results and Discussion

Working electrode compositions for NO analysis have spanned many materials including carbon ink,[59] gold/indium tin oxide,[64] and platinum.[48, 65] Platinum (Pt) working electrodes were utilized for this study due to availability, compatibility with our microfabrication equipment, and inherent robustness for sensor applications. Working electrodes were deposited by metal evaporation using standard photolithographic techniques. Clean glass was first modified with a thin (10 nm) layer of Ti to improve the adhesion of Pt at the desired thickness (150 nm), with metal thickness monitored using a quartz crystal microbalance.

Prior to xerogel modification, an ethanol-resistant photoresist (1002F-50) mask was applied over the entire substrate to enable selective deposition of the membrane solution over only the working electrodes after UV exposure and processing. To ensure selectivity for NO over interfering species, a 20% (v/v) 17FTMS-MTMOS fluorinated alkoxysilane xerogel membrane was deposited onto the microfabricated working electrodes. Selectivity for NO using xerogel sensor membranes was modified slightly from what we reported previously for Pt-coated tungsten conical wire electrodes.[47] Of note, spread-casting of the sol was necessary to enable reproducible coating of the planar Pt electrodes; dip-coating of this substrate (in sol) did not allow for sufficient control over the ensuing xerogel thickness. The spread-casting process consistently produced xerogel membranes that were 129 ± 59 nm thick, robust (i.e., scratch resistant) and capable of withstanding subsequent solution immersion (for use as sensors) without delamination or cracking of the films.

Before microfluidic device fabrication, the xerogel-coated Pt electrodes were characterized with respect to NO sensitivity and selectivity over common interferents in a stirred solution of PBS. An unforeseen benefit of the cast NO-selective membrane was reduced background signal and noise while making measurements. While the sensitivity of the membrane-coated Pt electrodes to NO was reduced by ~10% relative to bare electrodes (2.2 to 2.0 pA nM^{-1} NO, respectively), the decreased noise allowed for an improved limit of detection (260 vs. 6 nM NO for bare vs. xerogel-coated, respectively). Analogous to our previous wire-based electrodes,[47] the sensitivity of the xerogel-modified electrodes to NO was ~4 orders of magnitude greater than most of the interferents tested (nitrite, ascorbic acid, acetaminophen, uric acid, hydrogen sulfide, ammonia/ammonium, peroxynitrite).

A microfluidic device was fabricated by placing a glass substrate patterned with a Ag reference electrode on top of a ~3 mm wide microfluidic channel formed by applying two strips of double-sided Kapton® polyimide tape (~90 μm thick) across the working electrode substrate. A cutaway illustration of the device fabricated in the manner is shown in Figure 1. A deep, wide channel was chosen for this design to allow for adequate flow of more viscous biological fluids like blood or plasma. The addition and removal of sample were accomplished by fixing glass (8 mm diameter) reservoirs over the inlet and outlet vias with epoxy.

The fully-assembled device was characterized using constant potential amperometry at a working electrode potential of +700 mV vs. Ag/AgCl pseudo-reference/counter electrode. To achieve a steady baseline current, the device was polarized in PBS for ~1 h prior to testing. Nitric oxide calibration curves were constructed by adding 1.6 μL aliquots of saturated NO to a PBS solution and transferring ~1 mL of this solution to the sample inlet reservoir of the device. Measurements were recorded upon stabilization of the oxidation current. The NO solution in the reservoir was then replaced with another NO solution of a different concentration. As shown in Figure 2, the response to NO for bare and membrane-coated electrodes in the microfluidic device geometry was 2.0 and 1.4 pA nM^{-1} NO, respectively. As would be expected, the xerogel-coated electrode was characterized by a lower sensitivity than the bare electrode due to slowed NO diffusion across the membrane to the electrode surface. In addition, sensor response to NO for both the bare and coated electrodes was lower for the microfluidic devices relative to the entire glass substrate (described previously) because the channel exposes only a portion of the actual working electrode area patterned onto the glass.

Despite lower sensitivity when encased within the microfluidic device, the limit of detection for both the bare and coated microfluidic electrodes were 880 and 840 pM NO, roughly 1 log lower than the same electrodes prior to device fabrication. The improved limit of detection is attributed to lower noise due to the elimination of bulk convection and oscillating magnetic field from the stir plate. Furthermore, the use of gravity flow avoids pulsatile noise common to peristaltic pumps. For the device configuration described, volumes as low as 250 μL were adequate for successful NO analysis. By integrating a pulsatile-free flow control device (e.g., a venturi or syringe pump) and/or reducing channel width, even smaller volumes are conceivable. The response of the xerogel-coated electrode to nitrite, ascorbic acid, acetaminophen, uric acid, hydrogen sulfide, ammonium, ammonia, and peroxynitrite (both protonated and deprotonated) was exceptionally low. The difference in selectivity between bare and xerogel-coated electrodes is provided in Table 1. Of note, an improvement in selectivity over most interferents was observed using the xerogel membrane. The presence of ammonia was the exception, although the response to ammonia is of minimal concern as this species would not be present at high concentrations at physiological pH (7.4).

Microfluidic NO sensor response in physiological fluids

The analytical performance (i.e., sensitivity and selectivity) of the microfluidic NO sensor was characterized in wound fluid and whole blood to determine clinical analysis potential. Despite the presence of proteins, the microfluidic NO sensor proved capable of measuring NO in simulated wound fluid (10% FBS in water, v/v, based on the composition of interstitial fluid), a clinically relevant sample for which NO analysis may prove useful due to NO's role in wound healing.[10–12, 66] Boykin recently suggested that NO could be used as a prognostic biomarker for assessing wound healing if easily measured in wound extracts.[66] The microfluidic sensor responded to NO additions in the simulated wound fluid sample with a LOD of 18 nM, roughly 20 times poorer than in PBS. The increased NO detection limit is attributed to NO scavenging, as would be expected for proteinaceous solutions. Indeed, the LOD was increased further in whole blood.

Measurement of NO in whole blood is believed to be difficult due to NO scavengers such as hemoglobin.[67–69] To calibrate NO sensitivity accurately, aliquots of a saturated NO solution were added to 1 mL samples of porcine blood prior to transfer into the microfluidic device. As shown in Figure 3, the addition of saturated NO solution was readily measurable, producing currents proportional to the amount of NO spiked into the blood up to 100 μM. Of note, care was taken to minimize the period between NO injection into the blood and the analysis to avoid degradation of the NO signal due to reaction with scavenging species present in the blood. As shown in Figure 3, the signal did decay over time (within ~100 s), indicating the prevalence of, and problems associated with, NO scavenging/loss.

Although the sensitivity to NO in blood was decreased relative to PBS (0.0035 vs. 1.4 pA nM^{-1} NO), the reduced noise characteristic of the microfluidic device configuration still enabled a satisfactory LOD (472 nM NO). A LOD of ~500 nM is likely sufficient for studying a number of NO-mediated disease states where NO concentrations have been reported in the μM range.[2, 3, 70–74] Of note, slightly greater sensitivities (0.0125 vs. 0.0035 pA nM^{-1} NO) were observed for larger NO concentration ranges (i.e., 20–100 μM NO). We attribute this response to the greater concentration of NO relative to potential scavengers in blood.

Nitric oxide levels in sepsis

Sepsis is a systemic inflammatory response caused by severe infection and characterized by a multifaceted immunologic response consisting of an initial hyperinflammatory phase and subsequent immunosuppression.[75–78] Due to NO's role in the immune response to pathogens,[17–19] previous studies have monitored plasma concentrations of nitrate and nitrite —both stable end products of NO oxidation in vivo—using the Griess assay to assess their role as biomarkers of sepsis. As expected, large concentration changes were observed for severely septic patients.[2, 3, 79] While indirect NO monitoring via the Greiss assay may provide some insight into changes in NO dynamics throughout the progression of disease, blood sample processing and poor LOD preclude bedside monitoring and/or sepsis risk assessment (at pre-severe disease levels). In contrast, the microfluidic NO sensor described herein may represent a strategy for point-of-care monitoring of NO directly in whole blood. To evaluate the ability to assess sepsis progression, we infected mice with a single but lethal (96% mortality within 48 h) dose of *P. aeruginosa* (2–4 x 10^7 colony-forming units). A group of unmanipulated animals (n=8) was used as the 0 h-time point to represent healthy or baseline blood NO concentrations. Blood was sampled from infected mice at 2, 6, and 24 h (n = 8, 10, and 13 animals per group, respectively) throughout the course of sepsis progression. As expected, blood NO concentration changes over 2, 6, and up to 24 h after introduction of bacteria were statistically significant, reaching 82 ± 12 μM at 24 h. This 8-fold increase agrees with those reported previously by indirect detection of NO_X

species.[2, 3, 79] For example, Strand et al. reported a 7-fold increase in average NO_X concentration in human patients with sepsis (144 ± 39 μM) relative to healthy patients (20 ± 3 μM).[2]

The observed large increase in blood NO in this study is not surprising given the lethal bacterial dose administered. Future experiments will employ a lower, less lethal dose of *P. aeruginosa* and smaller measurement intervals, if necessary, to study the onset of sepsis. Additionally, the effects of other bacterial strains and antibiotic treatment on blood NO levels will be assessed to more fully gauge the suitability of NO as a sepsis biomarker and prognosis indicator upon treatment.

Conclusions

Herein we describe the use of standard photolithographic microfabrication techniques to construct a microfluidic NO sensor. The use of a NO-selective working electrode and microfluidic geometry enable highly sensitive detection of NO in both PBS and more challenging biological matrices including simulated wound fluid and whole blood. The analytical performance of the microfluidic sensor was dependent on sample milieu, with excellent sensitivity and selectivity for NO in PBS. As expected, the response of the device to NO in biological fluids was attenuated due to scavenging of NO by proteins. Nevertheless, the 472 nM LOD in blood is the lowest reported to date using direct electrochemical detection. The microfluidic device configuration enables rapid analysis of NO at low concentrations and in small (~250 μL) sample volumes that may prove useful for studying NO's action as a potential disease biomarker and/or therapeutic. As an example, whole blood NO levels changed dramatically in a pneumonia mouse model of infection indicating NO's potential as a biomarker for sepsis.

Acknowledgments

The authors acknowledge research support from the National Institutes of Health (NIH NIAID A13-0212, GM072808 (CMC), and GM095442 (RM and BPY)). We also thank Professor Nancy Allbritton for providing 1002F-50 photoresist, Nicholas Batz for vapor deposition of APTES, and the Francis Owen Blood Lab for providing fresh porcine blood upon request.

References

1. Dudzinski DM, Igarashi J, Greif D, Michel T. Annu Rev Pharmacol Toxicol. 2006; 46:235–276. [PubMed: 16402905]
2. Strand ØA, Leone A, Geircksky KE, Kirkebøen KA. Crit Care Med. 2000; 28:2779–2785. [PubMed: 10966250]
3. Ochoa JB, Udekwu AO, Billiar TR, Curran RD, Cerra FB, Simmons RL, Peitzman AB. Ann Surg. 1991; 214:621–626. [PubMed: 1953116]
4. Ignarro, LJ. Nitric Oxide: Biology and Pathobiology. Academic Press; San Diego: 2000.
5. McCleverty JA. Chem Rev. 2004; 104:403–418. [PubMed: 14871130]
6. Thomas DD, Ridnour LA, Isenberg JS, Flores-Santana W, Switzer CH, Donzelli S, Hussain P, Vecoli C, Paolocci N, Ambs S, Colton CA, Harris CC, Roberts DD, Wink DA. Free Radical Biol Med. 2008; 45:18–31. [PubMed: 18439435]
7. Wink DA, Mitchell JB. Free Radical Biol Med. 1998; 25:434–456. [PubMed: 9741580]
8. Knowles RG, Moncada S. Biochem J. 1994; 298:249–258. [PubMed: 7510950]
9. Zhou L, Zhu DY. Nitric Oxide-Biol Ch. 2009; 20:223–230.
10. Luo JD, Chen AF. Acta Pharmacologica Sinica. 2005; 26:259–264. [PubMed: 15715920]
11. Isenberg JS, Ridnour LA, Espey MG, Wink DA, Roberts DD. Microsurgery. 2005; 25:442–451. [PubMed: 16044466]
12. Soneja A, Drews M, Malinski T. Pharmacological Rep. 2005; 57:108–119.

13. Donnini S, Ziche M. Antioxid Redox Sign. 2002; 4:817–823.
14. Morbidelli L, Donnini S, Ziche M. Curr Pharm Des. 2003; 9:521–530. [PubMed: 12570800]
15. Al-Ani B, Hewett PW, Ahmed S, Cudmore M, Fujisawa T, Ahmad S, Ahmed A. Plos One. 2006; 1:e25. [PubMed: 17183652]
16. Kuwabara M, Kakinuma Y, Ando M, Katare RG, Yamasaki F, Doi Y, Sato T. J Physiol Sci. 2006; 56:95–101. [PubMed: 16779917]
17. Fang FC. J Clin Invest. 1997; 99:2818–2825. [PubMed: 9185502]
18. Snyder SH, Bredt DS. Sci Am. 1992; 266:74–77.
19. Thomas DD, Ridnour LA, Isenberg JS, Flores-Santana W, Switzer CH, Donzelli S, Hussain P, Vecoli C, Paolocci N, Ambs S, Colton CA, Harris CC, Roberts DD, Wink DA. Free Radical Biol Med. 2008; 45:18–31. [PubMed: 18439435]
20. Privett BJ, Shin JH, Schoenfisch MH. Chem Soc Rev. 2010; 39:1925–1935. [PubMed: 20502795]
21. Bedioui F, Villeneuve N. Electroanalysis. 2003; 15:5–18.
22. Davies IR, Zhang XJ. Methods in Enzymol. 2008; 436:63–95. [PubMed: 18237628]
23. Hetrick EM, Schoenfisch MH. Annu Rev Anal Chem. 2009; 2:409–433.
24. Allen BW, Liu J, Piantadosi CA. Methods Enzymol. 2005; 396:68–77. [PubMed: 16291222]
25. Coneski PN, Schoenfisch MH. Chem Soc Rev. 2012; 41:3753–3758. [PubMed: 22362308]
26. Carpenter AW, Schoenfisch MH. Chem Soc Rev. 2012; 41:3742–3752. [PubMed: 22362384]
27. Riccio DA, Schoenfisch MH. Chem Soc Rev. 2012; 41:3731–3741. [PubMed: 22362355]
28. Zhou L, Zhu DY. Nitric Oxide-Biology and Chemistry. 2009; 20:223–230.
29. Gomes A, Fernandes E, Lima J. J Fluoresc. 2006; 16:119–139. [PubMed: 16477509]
30. Oblak TDA, Root P, Spence DM. Anal Chem. 2006; 78:3193–3197. [PubMed: 16643013]
31. Griess JP. Ber Dtsch Chem Ges. 1879; 12:426–429.
32. Archer S. FASEB J. 1993; 7:349–360. [PubMed: 8440411]
33. Mehta S, Javeshghani D, Datta P, Levy RD, Magder S. Crit Care Med. 1999; 27:385–393. [PubMed: 10075065]
34. Hurst RD, Clark JB. Sensors. 2003; 3:321–329.
35. Hetrick EM, Schoenfisch MH. Annu Rev Anal Chem. 2009; 2:409–433.
36. Hunter RA, Storm WL, Coneski PN, Schoenfisch MH. Anal Chem. 2013; 85:1957–1963. [PubMed: 23286383]
37. Brisby H, Ashley H, Diwan AD. Spine. 2007; 32:1488–1492. [PubMed: 17572616]
38. Brovkovych V, Stolarczyk E, Oman J, Tomboulian P, Malinski T. J Pharm Biomed Anal. 1999; 19:135–143. [PubMed: 10698575]
39. Brown FO, Finnerty NJ, Lowry JP. Analyst. 2009; 134:2012–2020. [PubMed: 19768208]
40. Dalbasti T, Kilinc E. Methods Enzymol. 2005; 396:584–592. [PubMed: 16291265]
41. Fan CH, Li GX, Zhu JQ, Zhu DX. Anal Chim Acta. 2000; 423:95–100.
42. Griveau S, Dumezy C, Seguin J, Chabot GG, Scherman D, Bedioui F. Anal Chem. 2007; 79:1030–1033. [PubMed: 17263331]
43. Hart CM, Kleinhenz DJ, Dikalov SI, Boulden BM, Dudley SC Jr. Methods Enzymol. 2005; 396:502–514. [PubMed: 16291257]
44. Malinski T, Mesaros S, Patton SR, Mesarosova A. Physiol Res. 1996; 45:279–284. [PubMed: 9085350]
45. Malinski T, Taha Z. Nature. 1992; 358:676–678. [PubMed: 1495562]
46. Oh BK, Robbins ME, Schoenfisch MH. Analyst. 2006; 131:48–54. [PubMed: 16365662]
47. Shin JH, Privett BJ, Kita JM, Wightman RM, Schoenfisch MH. Anal Chem. 2008; 80:6850–6859. [PubMed: 18714964]
48. Shin JH, Weinman SW, Schoenfisch MH. Anal Chem. 2005; 77:3494–3501. [PubMed: 15924380]
49. Vallance P, Patton S, Bhagat K, Macallister R, Radomski M, Moncada S, Malinski T. Lancet. 1995; 346:153–154. [PubMed: 7603231]
50. Zhang XJ. Front Biosci. 2004; 9:3434–3446. [PubMed: 15353368]

51. Cha WS, Anderson MR, Zhang FH, Meyerhoff ME. Biosens Bioelectron. 2009; 24:2441–2446. [PubMed: 19168347]
52. Zhang XJ, Cardosa L, Broderick M, Fein H, Lin J. Electroanalysis. 2000; 12:1113–1117.
53. Hughes MN, Centelles MN, Moore KP. Free Radical Biol Med. 2009; 47:1346–1353. [PubMed: 19770036]
54. Olson KR. BBA-Bioenergetics. 2009; 1787:856–863. [PubMed: 19361483]
55. Wang S, Lin X. Electrochim Acta. 2005; 50:2887–2891.
56. Frost MC, Meyerhoff ME. Curr Opin Chem Biol. 2002; 6:633–641. [PubMed: 12413548]
57. Yager P, Edwards T, Fu E, Helton K, Nelson K, Tam MR, Weigl BH. Nature. 2006; 442:412–418. [PubMed: 16871209]
58. Cai XX, Klauke N, Glidle A, Cobbold P, Smith GL, Cooper JM. Anal Chem. 2002; 74:908–914. [PubMed: 11866072]
59. Spence, Dana M.; Torrence, Nicholas J.; Kovarik, Michelle L.; Martin, Scott R. Analyst. 2004; 129:6.
60. Cha W, Tung YC, Meyerhoff ME, Takayama S. Anal Chem. 2010; 82:3300–3305. [PubMed: 20329749]
61. Pai JH, Wang Y, Salazar GTA, Sims CE, Bachman M, Li GP, Allbritton NL. Anal Chem. 2007; 79:8774–8780. [PubMed: 17949059]
62. Dominguez JA, Vithayathil PJ, Khailova L, Lawrance CP, Samocha AJ, Jung E, Leathersich AM, Dunne WM, Coopersmith CM. Shock. 2011; 36:381–389. 310.1097/SHK. 1090b1013e31822793c31822794. [PubMed: 21701422]
63. McConnell KW, McDunn JE, Clark AT, Dunne WM, Dixon DJ, Turnbull IR, DiPasco PJ, Osberghaus WF, Sherman B, Martin JR, Walter MJ, Cobb JP, Buchman TG, Hotchkiss RS, Coopersmith CM. Crit Care Med. 2010; 38:223–241. [PubMed: 19770740]
64. Andersson DI, Hughes D. Nat Rev Microbiol. 2010; 8:260–271. [PubMed: 20208551]
65. Hetrick EM, Shin JH, Stasko NA, Johnson CB, Wespe DA, Holmuhamedov E, Schoenfisch MH. ACS Nano. 2008; 2:235–246. [PubMed: 19206623]
66. Boykin JV. J Wound Ostomy Cont. 2010; 37:25–32.
67. Stamler JS, Simon DI, Osborne JA, Mullins ME, Jaraki O, Michel T, Singel DJ, Loscalzo J. Proc Natl Acad Sci. 1992; 89:444–448. [PubMed: 1346070]
68. Kim-Shapiro DB, Schechter AN, Gladwin MT. Arterioscler Thromb Vasc Biol. 2006; 26:697–705. [PubMed: 16424350]
69. Elsadek B, Kratz F. J Controlled Release. 2012; 157:4–28.
70. Brovkovych V, Stolarczyk E, Oman J, Tomboulian P, Malinski T. J Pharm Biomed Anal. 1999; 19:135–143. [PubMed: 10698575]
71. Sordillo JE, Webb T, Kwan D, Kamel J, Hoffman E, Milton DK, Gold DR. J Allergy Clin Immunol. 2011; 127:1165–1172. [PubMed: 21463890]
72. Parwani SR, Chitnis PJ, Parwani RN. IJDH. 2012; 10:67–73.
73. Ertekin V, Selimoglu MA, Turkan Y, Akcay F. J Clin Gastroenterol. 2005; 39:782–785. [PubMed: 16145340]
74. Sanchez A, Lukwiya M, Bausch D, Mahanty S, Sanchez AJ, Wagoner KD, Rollin PE. J Virol. 2004; 78:10370–10377. [PubMed: 15367603]
75. Hotchkiss RS, Karl IE. N Engl J Med. 2003; 348:138–150. [PubMed: 12519925]
76. Remick DG. Am J Pathol. 2007; 170:1435–1444. [PubMed: 17456750]
77. Stearns-Kurosawa DJ, Osuchowski MF, Valentine C, Kurosawa S, Remick DG. Annu Rev Pathol-Mech. 2011; 6:19–48.
78. Hotchkiss RS, Coopersmith CM, McDunn JE, Ferguson TA. Nat Med. 2009; 15:496–497. [PubMed: 19424209]
79. Kao CC, Bandi V, Guntupalli KK, Wu M, Castillo L, Jahoor F. Clin Sci. 2009; 117:23–30. [PubMed: 19105791]

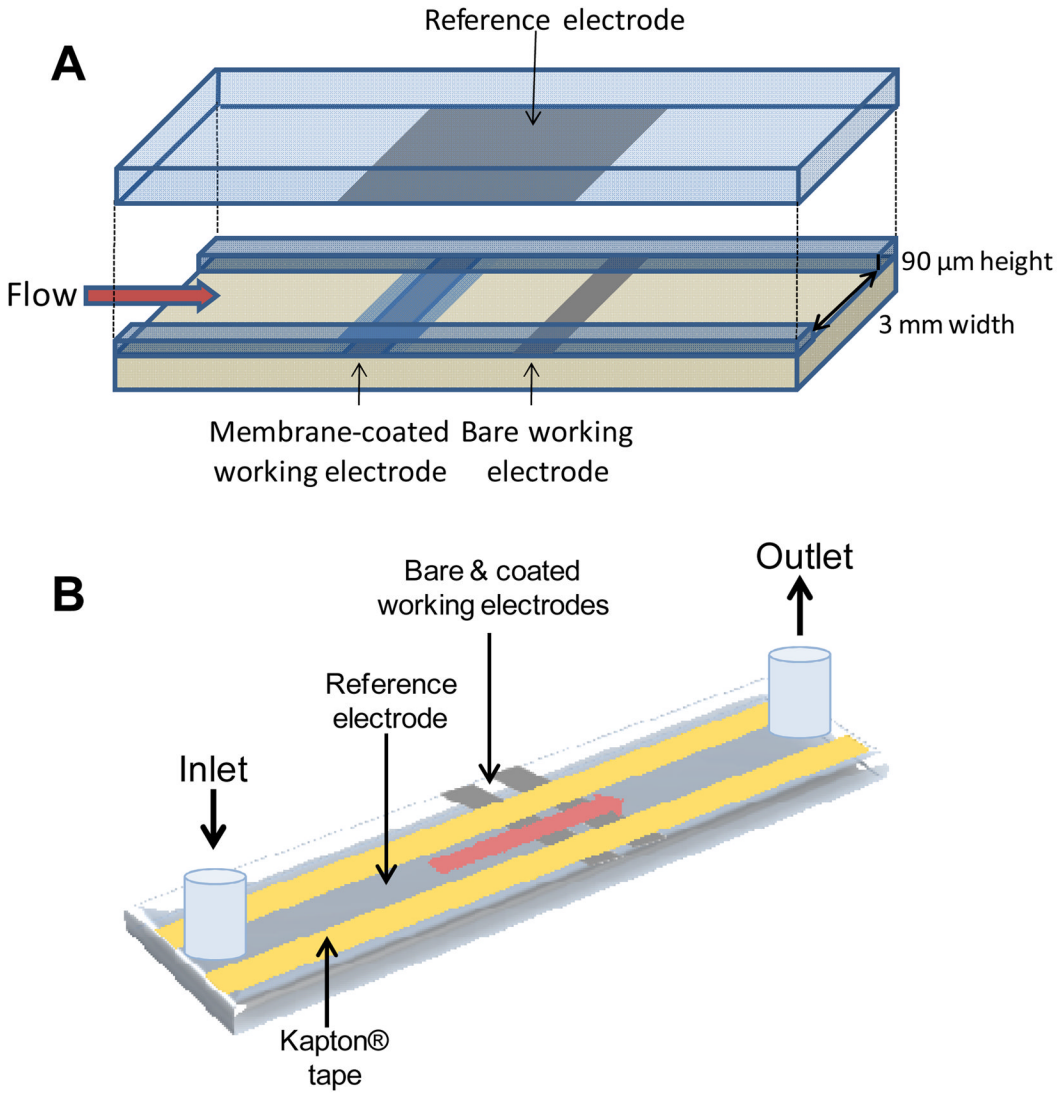

Figure 1.
A) Cutaway illustration of electrode locations and channel construction; and, B) fully assembled device with inlet and outlet reservoirs.

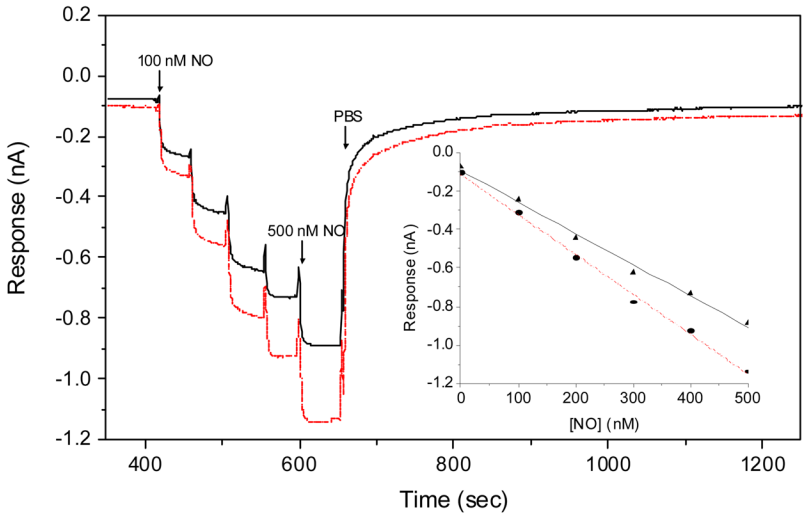

Figure 2.
Typical sensor response of bare (dotted red line) and xerogel-coated (solid black line) electrodes in microfluidic geometry to NO in PBS flowing at 15 μL/min. Inset shows NO calibration curves for bare (●) and xerogel-coated (▲) sensors.

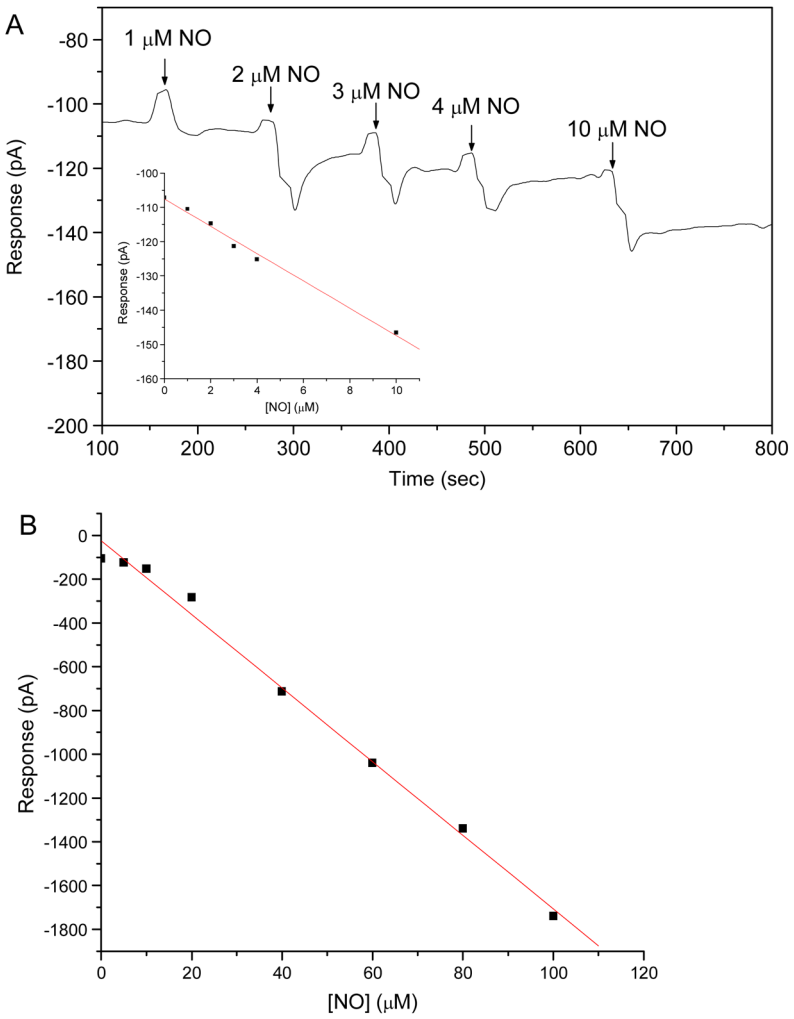

Figure 3.
Typcial microfluidic sensor response to 1 μM increases in NO concentration (A) and full dynamic range (B) in porcine whole blood.

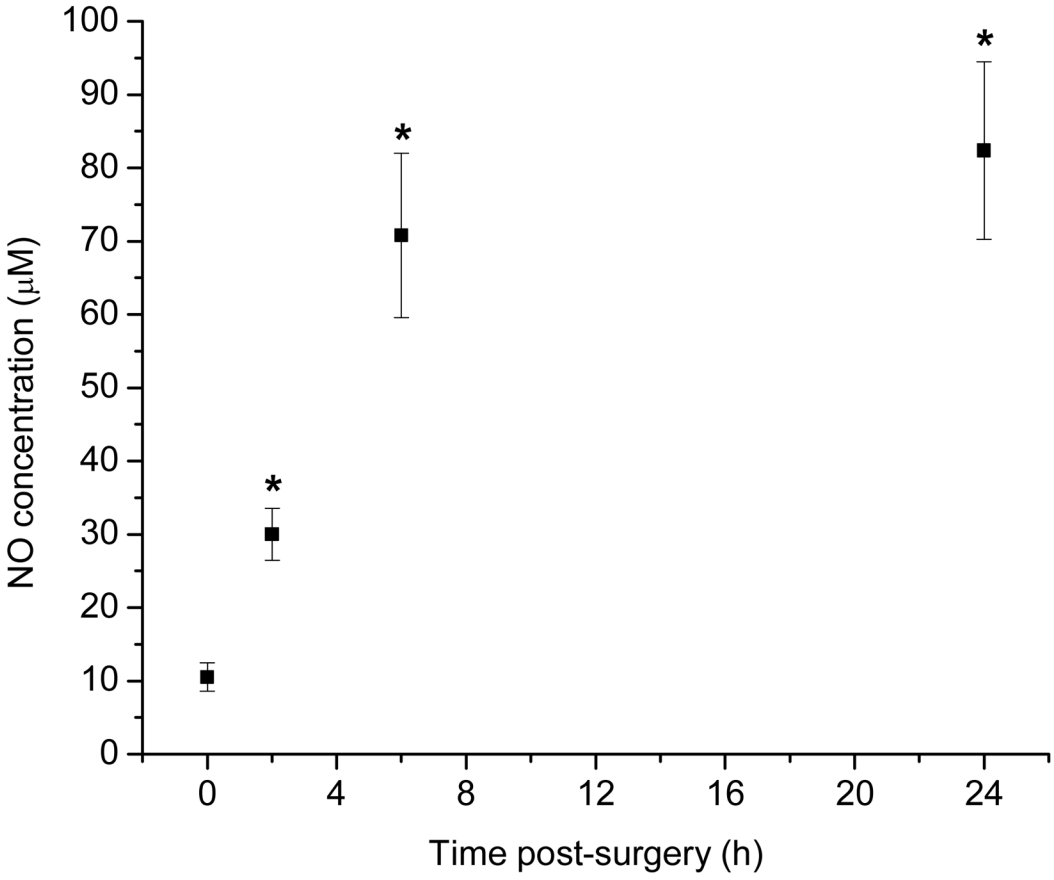

Figure 4.

Temporal changes in blood NO concentrations during the progression of sepsis in a pneumonia murine model of sepsis. Each data point represents the average ± standard error of the mean for a group of mice of $n \geq 8$. *denotes a significant difference in blood NO relative to the 0 h unmanipulated group ($p < 0.05$).

Table 1

Selectivity coefficients of common interferents for both bare and xerogel-coated platinum working electrodes.

Interferent	Selectivity (coated)	Selectivity (bare)
Hydrogen sulfide	< −6.0	−0.5
Ammonium	−5.8	−5.6
Nitrite	−5.3	−4.2
Uric acid	−5.0	−2.8
Ascorbic acid	−4.2	−2.4
Acetaminophen	−4.0	−2.7
Ammonia	−3.8	−3.8
Peroxynitrite (OONO-)	−4.0	−2.7
Peroxynitrite (OONOH)	−1.5	−0.5